Eur. Phys. J. B **45**, 243–248 (2005)
DOI: 10.1140/epjb/e2005-00052-4

THE EUROPEAN PHYSICAL JOURNAL B

All-optical probe of magnetization dynamics in exchange biased bilayers on the picosecond timescale

M.C. Weber[1,a], H. Nembach[1], S. Blomeier[1], B. Hillebrands[1], R. Kaltofen[2], J. Schumann[2], M.J. Carey[3], and J. Fassbender[4]

[1] Fachbereich Physik and Forschungsschwerpunkt MINAS, Technische Universität Kaiserslautern, Erwin-Schrödinger-Str. 56, 67663 Kaiserslautern, Germany
[2] Institut für Dünnschichtsysteme der Mikroelektronik, IFW Dresden, 01171 Dresden, Germany
[3] Hitachi Global Storage Technologies, San Jose Research Center, 650 Harry Rd., San Jose, CA 95120, USA
[4] Institut für Ionenstrahlphysik und Materialforschung, Forschungszentrum Rossendorf, 01314 Dresden, Germany

Received 9 September 2004 / Received in final form 14 October 2004
Published online 8 March 2005

Abstract. All-optical control of the magnetization of polycrystalline exchange bias bilayer systems is achieved using short picosecond laser pulses. Due to the photoexcitation, the spin temperature across the interface between the ferromagnetic and antiferromagnetic layer is elevated, resulting in a collapse of the interfacial exchange coupling. Thus, within the first 10 ps, a fast reduction of both the exchange bias field and the coercive field is observed for three different exchange bias systems comprising both different ferromagnets and antiferromagnets. The fast thermal unpinning is followed by a slower heat diffusion dominated relaxation process, which strongly depends on the thermal conductivity of the used buffer layers and substrates. The fast optical unpinning can be understood in terms of an internal anisotropy pulse field capable of triggering ultrafast precessional magnetization dynamics of the ferromagnetic layer, which makes heat-assisted coherent magnetization rotation feasible.

PACS. 75.70.Cn Magnetic properties of interfaces (multilayers, superlattices, heterostructures) – 75.30.Gw Magnetic anisotropy – 78.47.+p Time-resolved optical spectroscopies and other ultrafast optical measurements in condensed matter – 75.40.Gb Dynamic properties (dynamic susceptibility, spin waves, spin diffusion, dynamic scaling, etc.)

1 Introduction

Recently, significant effort has been focused on the development of magnetic media and methods to increase areal densities in magnetic recording above 1 Tb/in^2 [1]. One promising way is to make use of hybrid recording, e.g., by first lowering the magnetic anisotropy of a ferromagnetic storage medium by local laser heating and then changing the direction of the magnetization with a field pulse. This so-called "heat-assisted magnetic recording" [2] involves temperatures close to the Curie temperature of ferromagnetic films. It has been shown that short laser pulses are capable of creating hot, non-equilibrium spins, e.g., increasing the spin temperature of ferromagnets, on an ultrafast timescale [3]. The physics of ultrafast spin dynamics and especially precessional magnetization reversal in magnetic thin films are contemporary subjects, not only at a fundamental level but also of significant application interest, since data rates of 1 Gb/s are projected in the near future leading to fast switching times of 1 ns or even less.

Exchange biased bilayers represent an alternative system since the exchange bias anisotropy is known to depend strongly on temperature, however with temperatures involved far below the Curie temperature of typical ferromagnets. Active research has been directed towards a fundamental understanding of the origin of the unidirectional anisotropy in bilayers consisting of a ferromagnetic (F) and an adjacent antiferromagnetic (AF) layer [4–7]. The exchange bias effect is found, if the F-AF-bilayer is magnetic field cooled below the blocking temperature of the AF layer. The uncompensated AF spins are frozen with respect to the F layer spins. Thus, the interfacial AF spins cause an internal field, the so-called exchange bias field H_{eb}. This results in a shift of the ferromagnetic hysteresis loop with respect to zero applied field. In addition, due to the F/AF exchange coupling, the easy axis coercivity is enlarged compared to a single F layer.

In the present article, we address the dynamic response of the F/AF exchange coupling in polycrystalline

[a] e-mail: mweber@physik.uni-kl.de

exchange bias systems with special emphasis on magnetization unpinning due to picosecond laser excitations and to fast spin-lattice heating effects. Exchange biased bilayers represent ideal test material systems, since the exchange coupling at the F/AF interface is strongly temperature dependent in the region just below the blocking temperature T_B. This allows monitoring the spin temperature at the F/AF interface via the exchange bias shift field and the coercive field. Our aim is to investigate the time constants involved in the fast unpinning and recovery processes of the interfacial exchange coupling upon photoexcitation for different exchange biased systems based on different ferromagnetic and antiferromagnetic films. The picosecond photocontrol of the exchange coupling enables us to trigger heat-induced ultrafast precessional magnetization dynamics of the F layer magnetization showing the potential for ultrafast magnetization switching.

2 Experiment

Three different polycrystalline exchange bias bilayers with both different ferromagnetic and antiferromagnetic layers have been prepared. Samples of type I consist of a 5 nm thick $Ni_{81}Fe_{19}$ (F) and a 10 nm $Fe_{50}Mn_{50}$ (AF) layer on top of a 15 nm thick Cu buffer and a thermally oxidized Si substrate as a growth template. This top-pinned structure has been prepared by UHV electron beam and effusion cell evaporation. Finally, the samples were covered with a 2 nm Cr cap layer to prevent oxidation. For further details, see reference [8]. Planetary magnetron sputtering at room temperature has been used to prepare bottom-pinned samples of type II. A stack consisting of 5 nm Ta as a buffer, 20 nm $Ir_{25}Mn_{75}$ (AF), 6 nm $Co_{90}Fe_{10}$ (F) and a 5 nm Ta cap layer has been deposited on a glass substrate. Details can be found elsewhere [9]. A high vacuum multitarget magnetron sputtering system has been employed for the deposition of the bottom-pinned AF/F bilayer system of type III. On thermally oxidized Si substrates and 5 nm of Ta as growth templates 15 nm $Ni_{50}Mn_{50}$ (AF) and 4 nm $Co_{90}Fe_{10}$ (F) have been deposited together with an additional 4 nm Ta protective layer. Post-deposition annealing of type III samples leads to a chemically ordered FCT phase, which is antiferromagnetic [10]. Both FeMn and IrMn are antiferromagnetic also in the chemically disordered phase. Exchange bias for all sample types has been initialized by a magnetic field cooling procedure.

Exploiting the potential of a standard all-optical pump-probe setup with a picosecond mode-locked Nd:YVO_4 laser in combination with a SHG unit as a pulsed laser source, the optical control of the pinned magnetization is sensed in real time. All experiments have been performed with both a pump and probe pulse width of 8.5 ps, a pump pulse energy of $E_{pulse} = 11$ nJ, at a wavelength of 532 nm and a pump spot diameter of about 30 μm. Details of the setup can be found in reference [11]. A quasistatic hysteresis loop is sensed by a weak probe pulse (spot diameter 25 μm) in the longitudinal Kerr geometry with a fixed time delay to the laser excitation pulse, i.e., the loop then reflects the magnetic parameters present for a given pump-probe time delay.

3 Results

First, the prepared samples have been characterized quasistatically in order to deduce the temperature dependence of the exchange bias field. Easy axis hysteresis loops have been recorded for temperatures ranging from room temperature up to 400 °C. The shift field has been extracted from each loop according to $H_{eb} = (H_{c,left} + H_{c,right})/2$, where $H_{c,left}$ and $H_{c,right}$ represent the left and right coercive fields of the loops, respectively. The normalized shift field has been plotted as a function of temperature for all three sample types in Figure 1. The NiFe/FeMn and IrMn/CoFe bilayers show an initial shift field of $H_{eb} =$ 123 Oe and $H_{eb} = 700$ Oe and an initial easy axis coercivity of $H_c = 24$ Oe and $H_c = 90$ Oe, respectively. Samples of type III show a very small shift field of $H_{eb} = 20$ Oe but reveal a high coercive field of $H_c = 175$ Oe. The temperature dependence for type III samples is different from the dependence found for type I and II samples in the measured temperature window. Up to 200 °C the shift field for the NiMn based bilayers drops only about 10 percent, i.e., a plateau region exists, whereas FeMn and IrMn based bilayers reveal a monotonous decrease of the shift field with increasing temperature in the measured temperature range according to $(1 - T/T_B)^{-1}$. The NiFe/FeMn system exhibits a blocking temperature of $T_B = 155$ °C, while a blocking temperature for the IrMn/CoFe system of $T_B = 240$ °C can be deduced. For the NiMn/CoFe bilayer, the shift field disappears at $T_B = 400$ °C. All initial values such as shift and coercive fields and blocking temperatures are resumed in Table 1. The temperature dependence of the easy axis coercive fields of the respective sample types matches the temperature dependence found for the exchange bias shift fields. Figure 1 clearly proves the inherent temperature dependence of the exchange bias effect and is similar to previous results on exchange biased bilayer stacks based on different antiferromagnets [12].

Since the magnitude of the exchange bias and the easy axis coercive field is inherently related to the spin temperature, the exciting pump laser pulse is expected to serve as a "heating" pulse, thereby influencing the interfacial F/AF exchange coupling. In general, ultrashort laser pulses create a hot electron and spin system which is well thermalized within one picosecond [13]. The pump pulse duration in our setup is beyond this timescale, thus, only spin-lattice heating effects can be observed. Hence, the question arises whether we can make use of the observed strong temperature dependence on a picosecond timescale. Using the time resolved pump-probe scheme described above, the time evolution of the F/AF exchange coupling, e.g., the exchange bias field, upon photoexcitation has been recorded in easy axis geometry for the NiFe/FeMn system for pump-probe delay times up to about 3000 ps. Details of the experiment can be found elsewhere [11]. The transient exchange bias field $H_{eb}(t)$

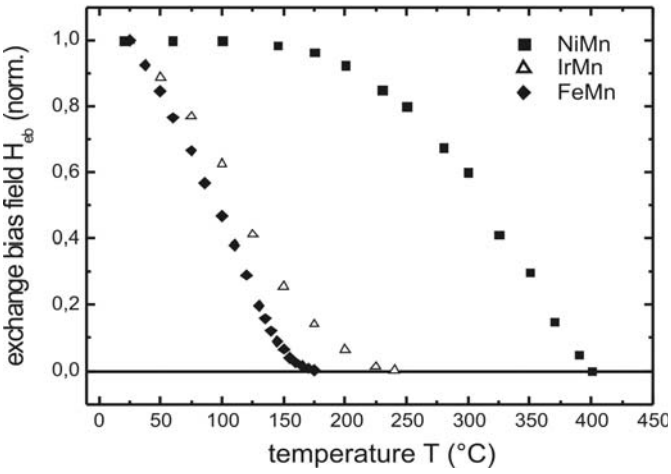

Fig. 1. Temperature dependence of the exchange bias shift field measured for the three prepared types of exchange bias samples. Easy axis hysteresis loops were recorded to evaluate the shift field. NiMn based bilayers (black squares) reveal a significant higher blocking temperature compared to FeMn (diamonds) and IrMn (open triangles).

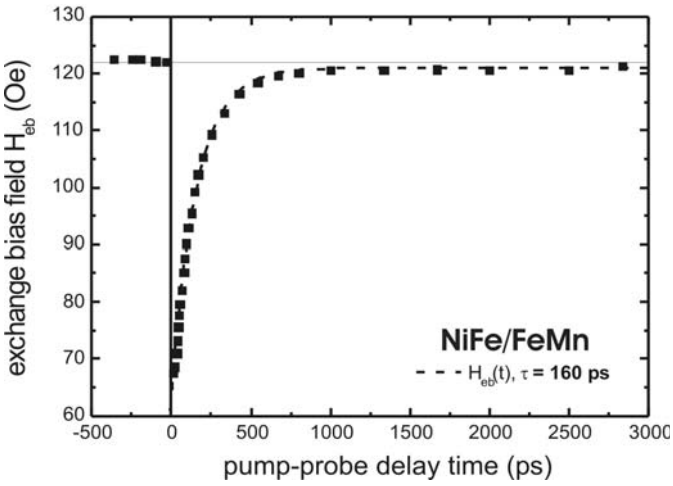

Fig. 2. Time evolution of the exchange bias field of an easy axis reversal loop for the NiFe/FeMn system. A model fit to equation (1) with the parameters $m = 0.45$ and $\tau = 160$ ps is shown by a dashed line.

Table 1. Summary of the initial shift fields H_{eb}, the coercive fields H_c and the blocking temperatures T_B of the different sample types. The measured modulation depths m and relaxation times τ are presented as well.

	NiFe/FeMn	IrMn/CoFe	NiMn/CoFe
T_B (°C)	155	240	400
H_{eb} (Oe)	123	700	20
H_c (Oe)	24	90	175
m	0.45	0.53	0.11
τ (ps)	160	205	183

from each hysteresis loop has been extracted in a similar way to the quasistatic case and is plotted as a function of pump-probe delay in Figure 2. Within the pump pulse width, i.e., within 10 ps the shift is reduced to about 50 percent of its initial value followed by a slower recovery. The measured data can be described by a phenomenological model [11], taking ultrafast thermal activation into account [14]

$$H_{eb}(t) = H_{eb}^{RT}(1 - m \cdot \exp(-t/\tau)), \qquad (1)$$

with the bias field H_{eb}^{RT} at room temperature, a modulation depth m and a relaxation time τ, comprising spin-lattice relaxation and predominantly heat diffusion effects. The best fit to our data is indicated by a dashed line in Figure 2 and yields $m = 0.45$ and $\tau = 160$ ps for the NiFe/FeMn type I samples. A detailed analysis of the time evolution of the easy axis coercivity reveals a relaxation behaviour similar to the time evolution of the shift field.

Next, it is addressed whether a photocontrol of the F/AF exchange coupling and the inherent temperature dependence can indeed account for the observed time evolutions. The time-resolved pump-probe scheme utilized for the FeMn (type I) based exchange bias system is used to trace the time evolution of the exchange bias field for the IrMn/CoFe (type II) bilayer as well. The transient hysteresis loops for different pump-probe delay times and the analysis of the transient shift field using equation (1) are summarized in Figure 3. Similar to the data of Figure 2, the shift field is reduced within the first 10 ps ($m = 0.53$) (see Fig. 3a) and relaxes back to its initial value with a time constant of $\tau = 205$ ps (see dashed line in panel 3b). Moreover, the time dependence of the easy axis coercivity of the IrMn/CoFe system again matches the one found for the shift field.

The time evolution of the exchange bias field deduced from these time-resolved MOKE measurements can be understood in terms of an internal anisotropy pulse field, which can trigger ultrafast precessional motion of the F layer magnetization [15,16]. Figure 4 exemplarily shows a magnetization precession trace of the CoFe macrospin with a frequency of $f = 13.2$ GHz. The working point for that time-resolved Kerr measurement is defined by applying a constant magnetic field of $H_{stat} = 515$ Oe, indicated by the black dot in Figure 3a, and varying the pump-probe delay continuously. The fast reduction of the shift field leads to a rapid change of the F layer magnetization equilibrium orientation, thus, to a torque on the magnetization. The observed high precession frequency reflects the large internal field acting on the F layer magnetization.

Finally, the all-optical measurement scheme has also been applied to samples of type III. The NiMn based exchange bias samples exhibit only a small shift field but a large easy axis coercivity. Due to the high blocking temperature of type III samples (see Fig. 1), only a small thermal influence on the shift field upon pump pulse application is expected. A small shift field makes the observation of small photoinduced changes difficult, hence, the

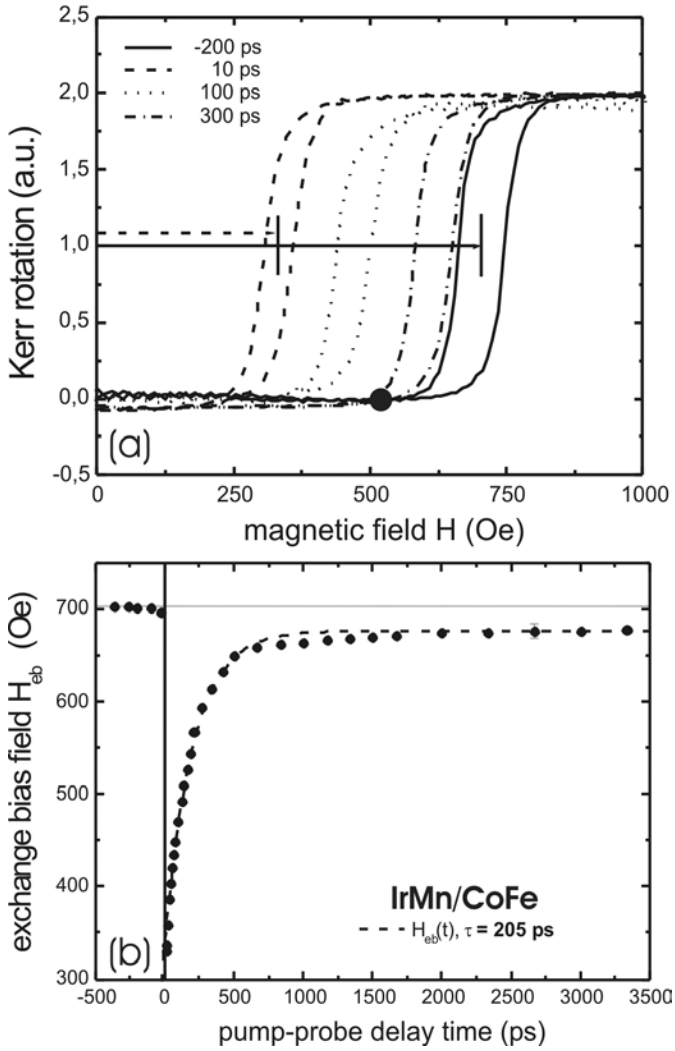

Fig. 3. Exchange bias shift field as a function of pump-probe delay measured for a IrMn/CoFe sample. (a) Easy axis transient hysteresis loops for various pump-probe delays as indicated. (b) Time evolution of H_{eb} with a Fit to equation (1) (see dashed line) yielding $\tau = 205$ ps and $m = 0.53$.

influence of the short laser excitation on the easy axis coercive field has been studied. For each pump-probe time delay the transient coercive field has been extracted according to $H_c = (H_{c,left} - H_{c,right})/2$ and was plotted as a function of pump-probe delay. Figure 5 summarizes both the measurement and real time analysis. The coercivity is reduced about 10 percent within the first 10 ps (see Fig. 5a) and recovers back to its initial value within a characteristic time τ (see dashed line in panel 5b). Again, the time constant involved is extracted by a fit to equation (1) which yields a relaxation time of $\tau = 185$ ps and $m = 0.11$. It is evident that equation (1) is capable of describing the photomodulation of the exchange coupling and, thus, the modulation of the coercivity in terms of ultrafast thermal activation.

Table 1 summarizes the measured initial values of the shift and coercive fields of the investigated sample types.

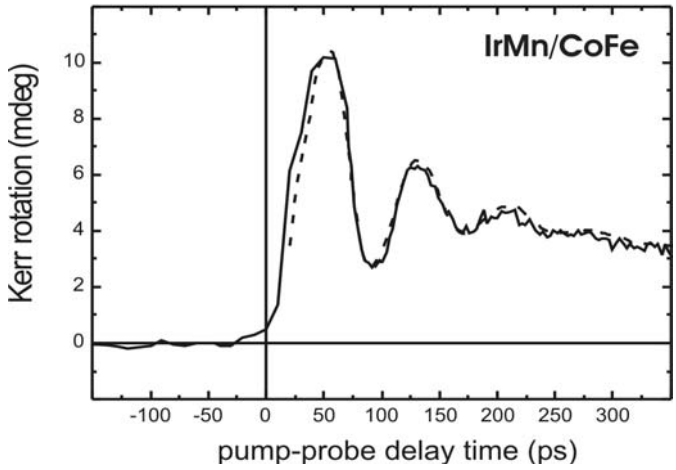

Fig. 4. High frequency (13.2 GHz) easy axis precession of the CoFe magnetization for an applied static field of $H_{stat} = 515$ Oe (see black dot in Fig. 3a). The dashed line is an exponentially damped sinusoid as guide to the eye.

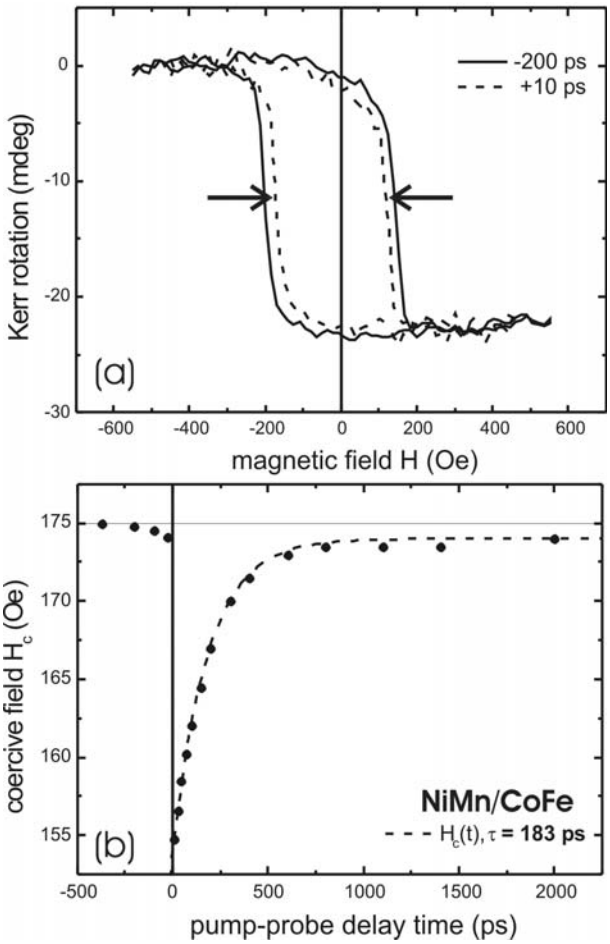

Fig. 5. Time dependence of the easy axis coercive field $H_c(t)$ for a NiMn/CoFe bilayer. (a) Easy axis transient loops for pump-probe delays of −200 and +10 ps. The black arrows highlight the reduction of the coercivity. (b) Time evolution of the coercivity with a fit to equation (1) (dashed line) yielding a relaxation time of 183 ps and a modulation depth of $m = 0.11$.

The internal relaxation times and modulation depths deduced from the all-optical measurements of the three sample types are presented as well.

The measured picosecond control of both the exchange bias shift field and the easy axis coercivity for different exchange bias systems indicates that the time evolutions rely on the mechanism of a fast unpinning and recovery of the interfacial exchange coupling.

4 Discussion and outlook

The underlying physical mechanism which accounts for the observed effects is based upon a sudden temperature increase and especially upon an elevated spin temperature. The measured quasistatic temperature dependence of the shift field $H_{eb}(T)$ presented in Figure 1 can be used to calibrate the spin temperature evolution upon laser excitation at the F/AF interface (exchange bias is mainly an interface effect). The respective reduction of the shift fields and coercive fields observed for the three sample categories can be translated into an absolute spin temperature. An equilibrium quantity such as temperature can be assigned in this case because the spin system equilibrates within a few tens of picoseconds. Typical spin-lattice relaxation times of ferromagnets are less than 80 ps [17]. A roughly 50 percent reduction of the shift field for the FeMn based bilayer yields an interfacial spin temperature of about 100 °C within the pump pulse width. In a similar way, a spin temperature of about 130 °C is found for the IrMn based samples. The 10 percent reduction of the easy axis coercivity in the case of NiMn/CoFe can be translated into a spin temperature of roughly speaking 140 °C. Slightly different values of both the heat capacity and the heat conductivity of the spin and lattice systems and slightly different light absorption coefficients of the respective materials within the laser penetration depth might account for the observed different, but comparable spin temperatures. However, care has to be taken with those equilibrium quantities within the first tens of picoseconds, since the spins are in non-equilibrium with the lattice on that timescale [17].

The sudden temperature increase within the first 10 ps leads to a collapse of the exchange coupling across the F/AF interface, resulting in a reduction of both the shift field and the easy axis coercivity. Upon photoexcitation, the ferromagnetic layer partially decouples from the antiferromagnetic layer, which leads to a thermally induced unpinning. Non-equilibrium conditions are achieved such that the magnetization reversal becomes isotropic [11]. Thus, the zero-field susceptibility shows a strong increase within the pump pulse width indicating that indeed a picosecond photocontrol of the exchange coupling turns out to be the underlying mechanism.

Currently, the reduction of the exchange bias and the coercive field for FeMn and IrMn based bilayer systems is limited to about 50% and the reduction of the coercivity for NiMn/CoFe to about 20% percent of the respective intial values. For larger pump pulse energies, irreversible processes occur which obstruct the stroboscopic measurement scheme used here. Since the investigated samples are polycrystalline, a distribution of different AF grain sizes is present. According to Takano et al. [18], large AF grains at the interface exhibit a smaller exchange coupling to the F spins across the interface. Upon laser excitation, these grains might already switch completely and will not relax to the original magnetization direction. In order to minimize the distribution width of exchange bias field values, measurements on epitaxial exchange bias systems are planned.

The ultrafast F/AF unpinning is followed by a slower relaxation of the shift field H_{eb} and the coercive field H_c back to their initial values. The recovery process comprises spin-lattice relaxation phenomena within the first tens of picoseconds accompanied by strong heat diffusion effects summarized by a phenomenological internal relaxation time. The fits of equation (1) to the measured time evolutions for all sample types yield comparable recovery times. However, there is a distinct difference for the respective sample types. The NiFe/FeMn samples exhibit the fastest internal relaxation time upon photoexcitation (τ = 160 ps), followed by the NiMn/CoFe system (τ = 183 ps) and the IrMn/CoFe exchange bias system (τ = 205 ps). The relaxation time for the slow recovery process can be understood in terms of energy dissipation, i.e., the spin and lattice systems are cooled by heat flow from the metallic bilayer to the substrate or to a region outside the laser spot, setting the ultimate limit for the speed of recovery. Spin-lattice based relaxation mechanisms can be expected to be independent of different exchange bias material systems. However, there is a significant influence of both the heat diffusion properties and Kapitza like phonon resistances of the buffer layers and substrates used on the relaxation process [19]. Only one dimensional heat flow has to be taken into account since the pump laser spot is much larger than the multilayer stack thickness. The values for the heat conductivity perpendicular to the sample surface of Ni, Fe, Ir, Mn and Co and the respective employed alloys are roughly within the same order of magnitude, but there is a significant difference for Ta and Cu buffer layers and especially for the utilized Si and glass substrates. A detailed heat diffusion analysis [19] can motivate the observed trend of the internal relaxation times of the respective sample classes. The combination of Cu as a buffer layer and a thermally oxidized Si substrate seems to speed up the relaxation time.

The obtained results indicate that a picosecond control of the free layer magnetization in spin-valve or TMR systems can be achieved by a photocontrol of the F/AF exchange coupling. The measured transient exchange bias and coercive fields can be interpreted in terms of an internal pulse field capable of triggering precessional motion of the F layer magnetization (see Fig. 4). The observed photomodulation of the exchange bias field for the presented example of a IrMn/CoFe system leads to a change of the equilibrium orientation of the F layer magnetization. A transient internal field is launched, which triggers precessional magnetization dynamics due to a torque following the initial "kick" on the F layer magnetization upon photoexcitation [16]. Thus, heat-induced coherent

precessional magnetization rotation or even ultrafast switching with internal anisotropy pulse fields and temperatures involved far below the Curie temperatures of single F layers become feasible.

5 Summary

It has been shown that picosecond short optical pulses can affect the magnetization reversal behaviour of exchange bias systems on a short picosecond timescale. The induced partial decoupling of the ferromagnetic layer from the antiferromagnet can even lead to a high frequency precessional response of the magnetization of the ferromagnetic layer. The internal relaxation time constants for FeMn, IrMn and NiMn based exchange bias bilayers turn out to be quite comparable. However, different heat conduction properties of the investigated material systems account for distinct differences of the speed of the internal relaxation process upon photoexcitation.

The authors would like to thank H.-J. Elmers for valuable discussions and Lumera Laser GmbH for supporting the laser equipment. One of the authors (M.C.W.) would like to acknowledge support by the Graduiertenkolleg 792 "Nichtlineare Optik und Ultrakurzzeitphysik" of the Deutsche Forschungsgemeinschaft. The work is supported by the European Communities Human Potential programs HPRN-CT-2002-00318 ULTRASWITCH and HPRN-CT-2002-00296 NEXBIAS.

References

1. R.W. Wood, J. Miles, T. Olsen, IEEE Trans. Magn. **38**, 1711 (2002)
2. J.J. Ruigrok, R. Coehoorn, S.R. Cumpson, H.W. Kesteren, J. Appl. Phys. **87**, 5398 (2000)
3. E. Beaurepaire, J.-C. Merle, A. Daunois, J.-Y. Bigot, Phys. Rev. Lett. **76**, 4250 (1996)
4. A.P. Malozemoff, Phys. Rev. B **37**, 7673 (1988)
5. J. Nogués, I.K. Schuller, J. Magn. Magn. Mater. **192**, 203 (1999)
6. R.L. Stamps, J. Phys. D: Appl. Phys. **33**, R247 (2000)
7. A.E. Berkowitz, K. Takano, J. Magn. Magn. Mater. **200**, 555 (1999)
8. S. Poppe, J. Fassbender, B. Hillebrands, Europhys. Lett. **66**, 430 (2004)
9. J.R. Childress, M.J. Carey, R.J. Wilson, N. Smith, C. Tsang, M.K. Ho, K. Carey, S.A. MacDonald, L.M. Ingall, B.A. Gurney, IEEE Trans. Magn. **37**, 1745 (2001)
10. S. Groudeva-Zotova, D. Elefant, R. Kaltofen, D. Tietjen, J. Thomas, V. Hoffmann, C.M. Schneider, J. Magn. Magn. Mater. **263**, 57 (2003)
11. M.C. Weber, H. Nembach, J. Fassbender, J. Appl. Phys. **95**, 6613 (2004)
12. G.W. Anderson, Y. Huai, M. Pakala, J. App. Phys. **87**, 5726 (2000)
13. J. Hohlfeld, E. Matthias, R. Knorren, K.H. Bennemann, Phys. Rev. Lett. **78**, 4861 (1997)
14. E. Fulcomer, S.H. Charap, J. Appl. Phys. **43**, 4190 (1972)
15. G. Ju, A.V. Nurmikko, R.F.C. Farrow, R.F. Marks, M.J. Carey, B.A. Gurney, Phys. Rev. Lett. **82**, 3705 (1999)
16. M. van Kampen, C. Josza, J.T. Kohlhepp, P. LeClair, L. Lagae, W.J.M. de Jonge, B. Koopmans, Phys. Rev. Lett. **88**, 227201-1 (2002)
17. A. Vaterlaus, T. Beutler, F. Meier, Phys. Rev. Lett. **67**, 3314 (1991)
18. K. Takano, R.H. Kodama, A.E. Berkowitz, W. Cao, G. Thomas, J. Appl. Phys. **83**, 6888 (1998)
19. M.C. Weber, H. Nembach, B. Hillebrands, J. Fassbender, IEEE Trans. Magn., in press